CARDIAC

CrossMark

Coronary CT angiography–derived plaque quantification with artificial intelligence CT fractional flow reserve for the identification of lesion-specific ischemia

Philipp L. von Knebel Doeberitz [1,2] · Carlo N. De Cecco [1] · U. Joseph Schoepf [1,3,4] · Taylor M. Duguay [1] ·
Moritz H. Albrecht [1,5] · Marly van Assen [1,6] · Maximilian J. Bauer [1] · Rock H. Savage [1] · J. Trent Pannell [1] ·
Domenico De Santis [1,7] · Addison A. Johnson [1] · Akos Varga-Szemes [1] · Richard R. Bayer [3] · Stefan O. Schönberg [2] ·
John W. Nance [1] · Christian Tesche [1,8]

Abstract

Objectives We sought to investigate the diagnostic performance of coronary CT angiography (cCTA)–derived plaque markers combined with deep machine learning–based fractional flow reserve (CT-FFR) to identify lesion-specific ischemia using invasive FFR as the reference standard.

Methods Eighty-four patients (61 ± 10 years, 65% male) who had undergone cCTA followed by invasive FFR were included in this single-center retrospective, IRB-approved, HIPAA-compliant study. Various plaque markers were derived from cCTA using a semi-automatic software prototype and deep machine learning–based CT-FFR. The discriminatory value of plaque markers and CT-FFR to identify lesion-specific ischemia on a per-vessel basis was evaluated using invasive FFR as the reference standard.

Results One hundred three lesion-containing vessels were investigated. 32/103 lesions were hemodynamically significant by invasive FFR. In a multivariate analysis (adjusted for Framingham risk score), the following markers showed predictive value for lesion-specific ischemia (odds ratio [OR]): lesion length (OR 1.15, $p = 0.037$), non-calcified plaque volume (OR 1.02, $p = 0.007$), napkin-ring sign (OR 5.97, $p = 0.014$), and CT-FFR (OR 0.81, $p < 0.0001$). A receiver operating characteristics analysis showed the benefit of identifying plaque markers over cCTA stenosis grading alone, with AUCs increasing from 0.61 with $\geq 50\%$ stenosis to 0.83 with addition of plaque markers to detect lesion-specific ischemia. Further incremental benefit was realized with the addition of CT-FFR (AUC 0.93).

Conclusion Coronary CTA–derived plaque markers portend predictive value to identify lesion-specific ischemia when compared to cCTA stenosis grading alone. The addition of CT-FFR to plaque markers shows incremental discriminatory power.

Key Points

• *Coronary CT angiography (cCTA)–derived quantitative plaque markers of atherosclerosis portend high discriminatory power to identify lesion-specific ischemia.*

✉ U. Joseph Schoepf
schoepf@musc.edu

1 Division of Cardiovascular Imaging, Department of Radiology and Radiological Science, Medical University of South Carolina, Charleston, SC, USA

2 Institute of Clinical Radiology and Nuclear Medicine, University Medical Center Mannheim, Medical Faculty Mannheim-Heidelberg University, Mannheim, Germany

3 Division of Cardiology, Department of Medicine, Medical University of South Carolina, Charleston, SC, USA

4 Heart & Vascular Center, Ashley River Tower, Medical University of South Carolina, 25 Courtenay Drive, Charleston, SC 29425-2260, USA

5 Center for Medical Imaging North East Netherlands, University Medical Center Groningen, University of Groningen, Groningen, The Netherlands

6 Department of Diagnostic and Interventional Radiology, University Hospital Frankfurt, Frankfurt, Germany

7 Department of Radiological Sciences, Oncology and Pathology, University of Rome "Sapienza", Rome, Italy

8 Department of Cardiology and Intensive Care Medicine, Heart Center Munich-Bogenhausen, Munich, Germany

• *Coronary CT angiography–derived fractional flow reserve (CT-FFR) shows superior diagnostic performance over cCTA alone in detecting lesion-specific ischemia.*
• *A combination of plaque markers with CT-FFR provides incremental discriminatory value for detecting flow-limiting stenosis.*

Abbreviations

AUC	Area under the curve
CAD	Coronary artery disease
cCTA	Coronary CT angiography
CT-FFR	Fractional flow reserve from coronary CT angiography
DSCT	Dual-source computed tomography
FFR	Fractional flow reserve
ICA	Invasive coronary angiography
NPV	Negative predictive value
OR	Odds ratio
PB	Plaque burden
PPV	Positive predictive value
RI	Remodeling Index
ROC	Receiver operating characteristics

Introduction

Invasive coronary angiography (ICA) with fractional flow reserve (FFR) measurement is the reference standard to assess the functional significance of coronary stenosis in patients with coronary artery disease (CAD) [1, 2]. Coronary CT angiography (cCTA) is an established method to rule out obstructive CAD. However, a purely anatomical evaluation has been shown to be a poor predictor in identifying the functional significance of a coronary lesion [3]. Plaque characterization and quantification derived from cCTA using semi-automatic software applications may enhance the performance of cCTA in predicting hemodynamically significant stenoses by providing plaque information beyond stenosis grading alone which may have impact on treatment decision making [4–8]. Recently, cCTA-derived fractional flow reserve (CT-FFR) using an on-site deep machine learning algorithm has been validated against invasive FFR for the determination of hemodynamically significant CAD [9–11]. Yet, the potential of cCTA-derived plaque quantification combined with CT-FFR for improved detection of lesion-specific ischemia deserves further study.

Thus, we sought to investigate the diagnostic performance of cCTA-derived plaque markers combined with deep machine learning–based CT-FFR to identify lesion-specific ischemia using invasive FFR as the reference standard.

Material and methods

Study population

This study was approved by the local Institutional Review Board with a waiver of informed consent and conducted in compliance with the Health Insurance Portability and Accountability Act (HIPAA). We retrospectively analyzed data of a patient cohort with suspected or known stable CAD who underwent cCTA followed by ICA with FFR measurement within 3 months between September 2008 and August 2017. Eighty-four out of the 85 patients included have been reported in a prior study by Tesche et al [12]. The prior study focused on a comparison of two different CT-FFR algorithms to predict hemodynamically significant CAD whereas the present study aims to detect cCTA-derived plaque markers combined with machine learning–based CT-FFR to identify lesion-specific ischemia. The patients' Framingham risk scores were calculated to reflect 10 year risk for cardiovascular events [12]. The indication for ICA was based on clinical parameters, response to therapy, cCTA data, and non-invasive functional test results according to clinical guidelines [13]. Patients with prior myocardial infarction, previous percutaneous coronary stent implantation, or coronary artery bypass grafting, severely reduced left ventricular function (ejection fraction ≤ 30%), and bifurcation stenoses were excluded from further analysis. Non-diagnostic cCTA image quality also led to exclusion. Covariates, including cardiac risk factors and patient baseline characteristics were obtained from medical records.

Coronary CTA acquisition

First, second, or third generation dual-source CT (DSCT) systems (SOMATOM® Definition, SOMATOM® Flash, or SOMATOM® Force, Siemens Healthineers) were used for image acquisition. Using the following parameters, patients underwent a non-contrast-enhanced coronary artery calcium scoring scan: 32 × 1.2 mm collimation, 120 kV tube voltage, 75 mA tube current, 3 mm section thickness in a 1.5 mm increment (first and second generation DSCT scanners); 44 × 1.2 mm collimation, 120 kV tube voltage, 80 mA tube current, 3 mm section thickness in a 1.5 mm increment (third generation DSCT scanner). cCTA acquisitions performed using the first generation DSCT were contrast-enhanced and retrospectively ECG-gated with the following parameters:

100–120 kV tube potential adapted to the patient's body mass index (BMI), 350–650 mAs tube current-time product, 0.28 s gantry rotation time, $2 \times 32 \times 0.6$ mm detector collimation with z-flying focal spot technique. Contrast enhancement was achieved using a biphasic injection protocol to administer 70–90 mL of contrast medium (Ultravist, 370mgI/mL iopromide, Bayer) at 4–6 mL/s, followed by a 30 mL saline flush. cCTA acquisitions performed using the second generation DSCT system contrast-enhance and prospectively ECG-gated with the following parameters: 80–120 kV tube potential adapted to the patient's BMI, 350–650 mAs tube current-time product, 0.28 s gantry rotation time, $2 \times 64 \times 0.6$ mm detector collimation with a z-flying focal spot. Contrast enhancement was achieved by injecting 50–80 mL of iopromide at 4–6 mL/s followed by a 30 mL saline bolus chaser. cCTA acquisitions performed using the third generation DSCT system were contrast-enhance and prospectively ECG-gated with the following parameters: 70-130 kV tube potential automatically selected using an automated tube-voltage selection algorithm (CARE kV, Siemens), 200–650 mAs tube current-time product, 0.25 s gantry rotation time, $2 \times 192 \times 0.6$ mm detector collimation with a z-flying focal spot. There was 40–70 mL iopromide injected at 4–6 mL/s followed by a 30 mL saline bolus chaser. Beta-blockers and nitroglycerine were used at the discretion of the attending physician of the day. Filtered back projection image reconstruction was performed in the cardiac phase with the least motion: temporal resolution of 83, 75, or 66 ms, section thickness of 0.75 mm, reconstruction increment of 0.4 or 0.5 mm and a smooth convolution kernel (B26f). Effective radiation dose was estimated by multiplying the dose-length-product by a chest-specific conversion coefficient ($k = 0.014$ mSv/Gy/cm).

Analysis of cCTA data and plaque quantification

cCTA datasets were analyzed on a post-processing workstation (syngo.via VB10, Siemens Healthineers) by two observers (C.T./C.N.D.C), who had 4 and 8 years of experience in cCTA analysis and were blinded to the patient histories. Each observer analyzed the lesion characteristics and a consensus interpretation with both observers was done for all discordant cases. Observers used transverse sections and automatically generated curved multiplanar reformations for their assessment. One target lesion per vessel, where invasive FFR was performed, was evaluated. The reference diameter, area stenosis determination, and average dimensions of non-affected vessel segments were measured immediately proximal and distal to the lesion of interest at points free of atherosclerotic plaque. Societal guidelines using the coronary artery disease reporting and data system (CAD-RADS™) were used to determine the degree of stenosis: (1) none (0%) or minimal (1–24%), (2) mild (25–49% stenosis), (3) moderate (50–69%

stenosis), (4) severe (70–99% stenosis), (5) total occlusion (100%). Obstructive CAD was defined as $\geq 50\%$ stenosis [14].

Plaque burden (PB in %) was measured in the following manner: PB = [plaque area/vessel area] $\times$ 100. On vessel cross-sections, remodeling index (RI) was measured as the ratio of the vessel area of the lesion over the proximal luminal reference area [15]. The presence of napkin-ring sign, described as a low attenuating plaque core circumscribed by area of higher attenuation, was assessed [16]. Spotty calcifications were visually assessed as calcifications covering < 90° of the vessel circumference while being > 3 mm length [17].

A dedicated semi-automatic software prototype (Coronary Plaque Analysis 4.2.0 syngo.via FRONTIER, Siemens Healthineers) was used for plaque quantification as previously described [18, 19]. Briefly, the software uses automated segmentation based on attenuation values prevailing in the target anatomy within user-defined proximal and distal boundaries to compute quantitative plaque descriptors. The beginning and end of a lesion of interest was defined as the proximal and distal points that were free of atherosclerotic changes. Lesion length, total plaque volume, and calcified and non-calcified plaque volume were automatically measured by the software (Fig. 1). The analysis software used the following boundary values (HU): lipid-rich (17–70), fibrotic (71–124), vessel lumen (125–511), and calcified (> 511) [20].

CT-FFR determination

CT-FFR calculations were performed using a deep machine learning software prototype (Siemens cFFR, Version 2.1, Siemens, currently not commercially available) as previously described [10, 21]. This algorithm resides on a regular workstation and with physician input, creates a patient-specific anatomical model of the coronary tree in a semi-automated fashion. The algorithm is based on a deep learning framework to integrate the complex non-linear relationship between the various features extracted from the coronary tree geometry and to compute the functional severity of the lesion. The deep learning algorithm employs a multilayer neural network architecture that was trained offline against a computational fluid dynamics simulation to learn the complex relationship between the anatomy of the coronary tree and its corresponding hemodynamics. Model training was performed using a large database of 12,000 synthetically generated coronary anatomies and their corresponding hemodynamic conditions from a computational fluid dynamics simulation. Based on geometric features (i.e., vessel radius, degree of tapering, and branch length) of the patient's coronary anatomy on cCTA, the algorithm uses the learned relationship to calculate the machine learning based CT-FFR values. The quantity of interest, e.g., FFR, is represented by a model built from a database of samples with known characteristics and outcome derived from the
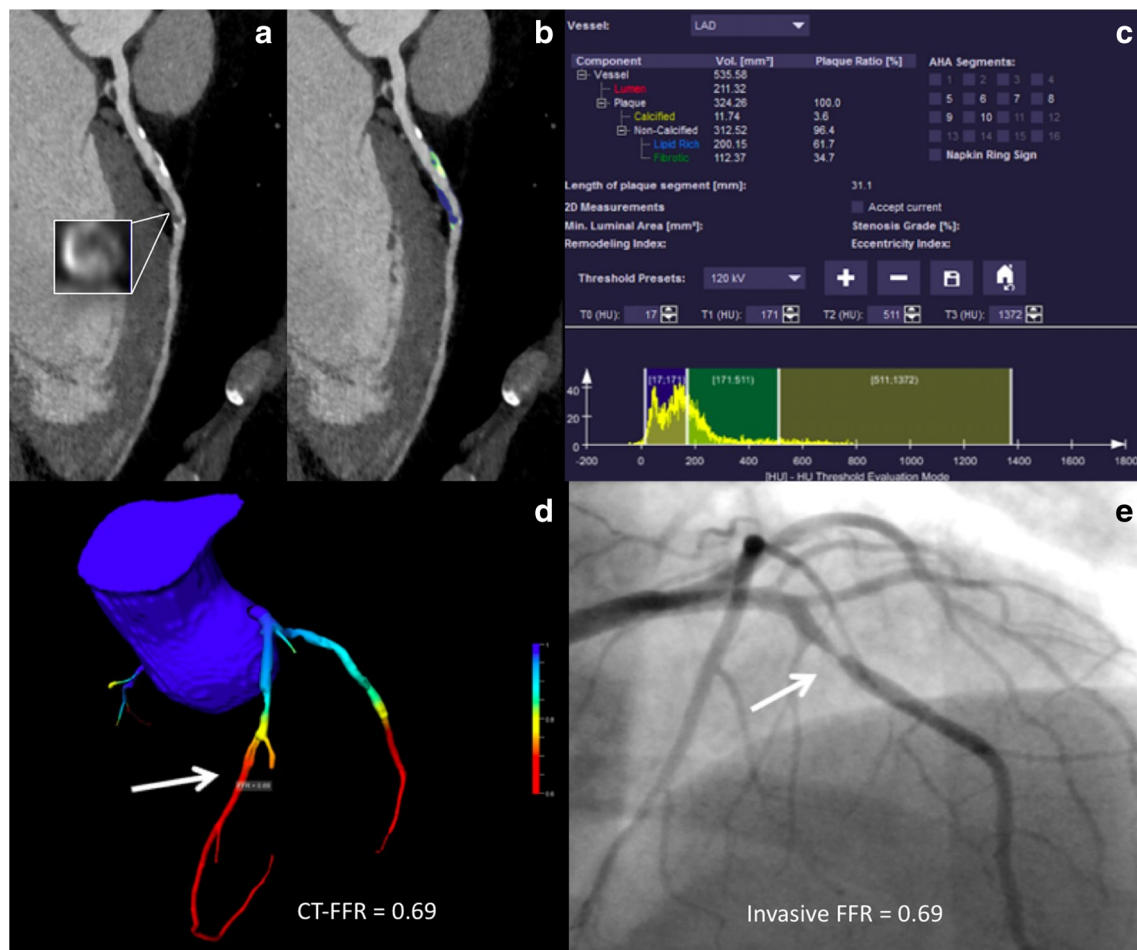
Fig. 1 Case example of coronary stenosis on cCTA, cCTA-based plaque analysis, CT-FFR determination, and ICA with FFR measurement. 64-year-old man who had undergone cCTA for suspected CAD. **a** cCTA demonstrated stenotic plaque of the LAD (arrow) showing a contrast-enhanced rim (positive napkin-ring sign). **b, c** Color-coded semi-automatic plaque quantification of the lesion shows the mixed plaque composition (calcified and non-calcified). **d** 3-dimensional color-coded mesh reveals a CT-FFR value of 0.69, indicating lesion-specific ischemia (arrow). **e** ICA shows obstructive stenosis (solid arrow) with invasive FFR of 0.69, confirming lesion-specific ischemia

computational fluid dynamic approach. For any point available within the coronary tree, CT-FFR values are derived by computing the ratio of the average local pressure over a cardiac cycle to the average aortic pressure, resulting in a color-coded 3-dimensional mesh throughout the coronary tree allowing for the determination of the CT-FFR value at arbitrary locations. Lesion-specific ischemia was defined as CT-FFR ≤ 0.80, as previously described [22].

ICA and FFR measurement

ICA was performed according to societal guidelines [23]. Each coronary segment was visually evaluated and quantitative coronary angiography measurement of the coronary lesions was obtained by the performing interventional cardiology team. Invasive FFR determination was obtained in cases of intermediate stenoses or lesions suspect for CAD at the discretion of the interventionalist. A pressure wire (Aeris, St. Jude Medical) was used to obtain baseline and hyperemic

gradients using a continuous infusion of intravenous adenosine (140 µg/kg/min). An FFR value ≤ 0.80 was considered diagnostic for lesion-specific ischemia [3]. In patients with two or more lesions suspected to be hemodynamically relevant, FFR measurements were performed on each lesion of interest. Co-registration of the location of invasive FFR measurement and the CT-FFR measurements was performed by an independent reviewer (J.W.N.) with > 10 years of experience in cardiovascular imaging by identifying the invasive FFR sample location on the fluoroscopic images and the corresponding location on the cCTA images using anatomic landmarks.

Statistical analysis

MedCalc (MedCalc Software, version 15) was used for all statistical analyses. Continuous variables are displayed as mean ± standard deviation or median with interquartile range when not normally distributed. Normal distribution was

assessed using Kolmogorov-Smirnov testing. Student t test and Mann-Whitney U test were used for parametric or non-parametric data. A multivariable logistic regression analysis (adjusted for Framingham risk score) was performed with cCTA-derived markers and CT-FFR as independent variables to identify possible independent predictors of lesion-specific ischemia with invasively measured FFR ≤ 0.80 as a dichotomous outcome. Variables that were significant in a univariate analysis were entered into the multivariable logistical regression model. A receiver operating characteristics (ROC) analysis was used to analyze performance for detecting hemodynamically significant stenosis. For the evaluation of discriminatory power, the area under the ROC curve (AUC) was measured according to the method of DeLong [24]. The Youden index derived from ROC curve analysis was used to determine the optimal threshold. Sensitivity, specificity, positive predictive value (PPV), and negative predictive value (NPV) were measured and presented with a 95% confidence interval. A stepwise model of ROC curves was used to evaluate the prognostic value of ≥ 50% stenosis on cCTA, combination of plaque markers, and CT-FFR. Model performance of increasing numbers of predictors was compared using the Wald test. Statistical significance was assumed with a p value ≤ 0.05.

Results

Patient characteristics

A total of 156 patients who had undergone ICA with FFR measurement and cCTA within 3 months were retrospectively analyzed. Twenty-two patients (13%) with prior myocardial infarction, 32 patients (19%) with previous revascularization in the vessel of interest, 9 (5%) patients with severely reduced left ventricular function, and 9 (5%) patients whose cCTA had insufficient image quality were excluded. A total of 84 patients (61 ± 10 years, 65% male) with 103 coronary lesions were eventually included. Additional baseline characteristics are presented in Table 1.

ICA with FFR measurement and cCTA

Out of the 103 coronary lesions, 32 lesions (31%) demonstrated lesion-specific ischemia with invasive FFR ≤ 0.80. The remaining 79 lesions (69%) were not hemodynamically significant (invasive FFR > 0.80). cCTA described obstructive CAD in 76 out of 103 lesions (74%). Out of these 76 lesions, 30 lesions (39%) were hemodynamic significant by invasive FFR measurement. Further procedural results are displayed in Table 2.

Table 1 Patient demographics. Total patient cohort ($n = 84$)

Age (years)	61 ± 10
Male sex n (%)	55 (65%)
Height (cm)	171 ± 11
Weight (kg)	88 ± 20
Body mass index (kg/m²)	31 ± 7
Cardiovascular risk factors	
Hypertension n (%)#	58 (69%)
Diabetes n (%)¶	27 (32%)
Dyslipidemia n (%)*	42 (50%)
Tobacco abuse n (%)	22 (26%)
CAD family history n (%)	28 (33%)
Framingham risk score (%)	21.3 ± 10
Medication at time of admission	
Aspirin n (%)	23 (27%)
Statins n (%)	35 (42%)
Beta-blocker n (%)	25 (30%)
Antidiabetics n (%)	27 (32%)
Diuretics n (%)	19 (22%)
ACE inhibitors n (%)	33 (39%)

CAD coronary artery disease, *ACE* angiotensin-converting enzyme

Defined as blood pressure > 140 mmHg systolic, > 90 mmHg diastolic, or use of antihypertensive medication

¶ Defined as an HbA1c of ≥ 6.5% or use of antidiabetic medication

*Defined as a total cholesterol of > 200 mg/dl or use of lipid-lowering medication. Data presented as mean ± standard deviation or numbers with percentages (%)

Association of plaque markers, CT-FFR, and lesion-specific ischemia

Total plaque volume, calcified plaque volume, plaque burden, spotty calcification, and Agatston calcium score showed no significant differences between hemodynamically significant and non-significant lesions with a trend of higher total plaque volume and plaque burden in ischemia-inducing lesions (Table 3). In contrast, lesion length (median 23.3 vs. 18.5 mm), non-calcified plaque volume (median 141.3 vs. 113.8 mm³), remodeling index (median 1.12 vs. 1.03), napkin-ring sign (median 24 vs. 29), and CT-FFR (median 0.73 vs. 0.92) were significantly different in hemodynamically relevant stenoses compared to non-relevant stenoses (all $p < 0.05$) (Table 3).

In a multivariable logistics regression analysis, lesion length (OR 1.15, $p = 0.037$), non-calcified plaque volume (OR 1.02, $p = 0.007$), remodeling index (OR 1.20, $p = 0.031$), napkin-ring sign (OR 5.97, $p = 0.014$), and CT-FFR ≤ 0.80 (OR 0.81, $p < 0.0001$) were significant predictors of lesion-specific ischemia (Table 4). An ROC curve analysis was performed for cCTA-derived plaque markers and CT-FFR to evaluate their discriminatory power, showing statistically significant differences between hemodynamically

Table 2 Procedural results (84 patients with 103 coronary lesions)

Quantitative coronary angiography	
Number of lesions *n*	103
Left anterior descending artery *n* (%)	71 (69%)
Left circumflex artery *n* (%)	17 (17%)
Right coronary artery *n* (%)	15 (14%)
Proximal lesions *n* (%)	31 (30%)
Medial lesions *n* (%)	53 (51%)
Distal lesions *n* (%)	19 (18%)
Luminal stenosis ≥ 50% *n* (%)	79 (77%)
FFR ≤ 0.80 *n* (%)	32 (31%)
Coronary CT angiography with fractional flow reserve	
Luminal stenosis ≥ 50% *n* (%)	76 (74%)
CT-FFR ≤ 0.80 *n* (%)	33 (32%)
Agatston coronary calcium score	431 (126, 1039)
Heart rate (bpm)	68 ± 12
Dose length product (mGy*cm)	473 ± 52
Effective radiation dose (mSv)	6.4 ± 0.8

Data presented as mean ± standard deviation, numbers with percentages (%), or as medians with 25th and 75th percentile

significant lesions and non-flow obstructive stenoses. An ROC analysis for significant predictors for hemodynamically significant lesions resulted in the following: lesion length AUC 0.70 (95%CI 0.59–0.78), $p = 0.0002$; non-calcified plaque volume AUC 0.62 (95%CI 0.52–0.72), $p = 0.049$, remodeling index AUC 0.62 (95%CI 0.52–0.71), $p = 0.052$, napkin-ring sign AUC 0.67 (95%CI 0.57–0.76), $p = 0.007$, and CT-FFR AUC 0.89 (95%CI 0.82–0.95), $p < 0.0001$. An ROC curve analysis with the optimal thresholds to identify lesion-specific ischemia and the calculated sensitivity, specificity, PPV, and NPV is shown in Fig. 2 and Table 5.

For these markers, different models of ROC curves were performed to evaluate the predictive value of a combination of markers in a stepwise fashion. A combination of plaque

Table 4 Multivariable logistic regression analysis of cCTA-derived plaque markers and CT-FFR

Parameter	Odds ratio	95%CI of odds ratio	*p* value
Lesion length > 21 mm	1.147	1.008–1.305	0.037
Non-calcified plaque volume > 132 mm³	1.016	1.004–1.028	0.007
Remodeling index > 1.03	1.201	1.102–1.323	0.031
Napkin-ring sign	5.965	1.438–24.731	0.014
Stenosis ≥ 50%	3.750	1.179–11.928	0.062
CT-FFR ≤ 0.80	0.809	0.737–0.888	< 0.0001

Adjusted for Framingham risk score

markers (lesion length, remodeling index, non-calcified plaque volume, and napkin-ring sign) added to stenosis ≥ 50% (AUC 0.61) improved the predictive value over stenosis ≥ 50% alone (AUC 0.83, $p = 0.0001$). The addition of CT-FFR ≤ 0.80 to stenosis ≥ 50% + plaque markers further enhanced prediction with incremental discriminatory power (AUC 0.93, $p = 0.031$). The AUC of CT-FFR alone was not improved with the addition of stenosis ≥ 50% and plaque markers (AUC 0.89 vs. 0.86, $p = 0.57$) (Fig. 3).

Discussion

Our results demonstrate that cCTA-derived plaque markers and CT-FFR have discriminatory power to differentiate between hemodynamically significant and non-significant coronary lesions. Lesion length, non-calcified plaque volume, remodeling index, and napkin-ring sign were significant predictors for lesion-specific ischemia over visual stenosis grading on cCTA alone with incremental predictive value with the addition of CT-FFR to these plaque markers.

Table 3 Analysis of cCTA-derived plaque markers and CT-FFR according to lesion-specific ischemia as defined by invasive FFR
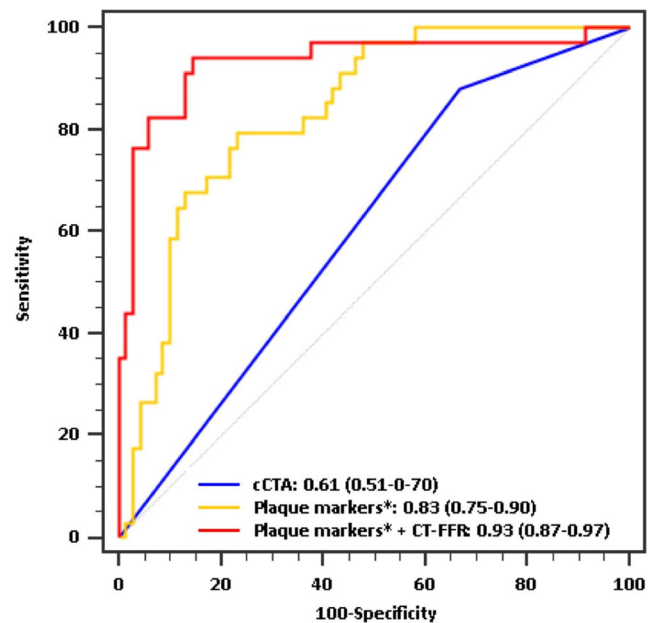
Parameter	All lesions *n* = 103	Lesions FFR > 0.80 *n* = 71	Lesions FFR ≤ 0.80 *n* = 32	*p* value
Lesion length (mm)	19.8 (16.4, 24.6)	18.5 (14.4, 22.6)	23.3 (19.9, 25.9)	0.001
Total plaque volume (mm³)	124.3 (79.0, 163.2)	106.5 (77.4, 148.9)	147.3 (97.6, 215.1)	0.081
Calcified plaque volume (mm³)	7.2 (3.2, 10.6)	8.1 (3.4, 11.0)	6.2 (2.5, 8.7)	0.57
Non-calcified plaque volume (mm³)	124.8 (94.6, 164.3)	113.8 (84.0, 145.7)	141.3 (96.6, 267.8)	0.011
Plaque burden (%)	55.4 (41.6, 71.5)	46.3 (34.3, 70.5)	64.0 (49.9, 72.3)	0.076
Remodeling index	1.06 (0.95, 1.15)	1.03 (0.94, 1.13)	1.12 (1.05, 1.12)	0.009
Napkin-ring sign	53 (51%)	29 (41%)	24 (75%)	0.010
Spotty calcification	54 (52%)	34 (48%)	20 (63%)	0.18
Agatston calcium score	431.5 (126.0, 1039.0)	424.5 (136.0, 1033.0)	698.0 (84.0, 1225.0)	0.53
Stenosis ≥ 50%	76 (74%)	48 (68%)	28 (88%)	0.037
CT-FFR	0.87 (0.76, 0.93)	0.92 (0.85, 0.95)	0.73 (0.69, 0.77)	< 0.0001

Data presented as medians with 25th and 75th percentile in parentheses or percentages in parentheses (%)
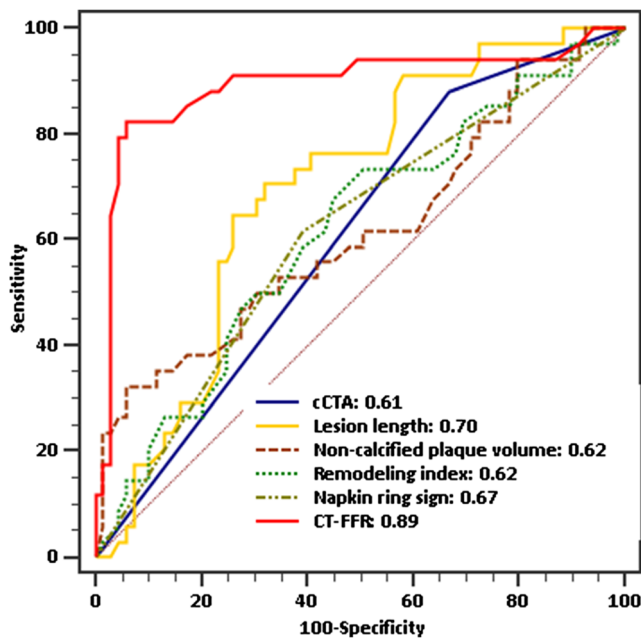
Fig. 2 Diagnostic performance of cCTA-derived plaque markers and CT-FFR for the identification of lesion-specific ischemia. ROC curve analysis is shown for visual stenosis grading (≥ 50% stenosis) for cCTA, lesion length, non-calcified plaque volume, remodeling index, napkin-ring sign, and CT-FFR for the discriminatory value of hemodynamically significant stenosis defined by invasive fractional flow reserve

Fig. 3 Comparison of different models for the prediction of lesion-specific ischemia defined by invasive fractional flow reserve. Stepwise model of receiver operating characteristic (ROC) curves for cCTA-derived plaque markers including ≥ 50% stenosis and CT-FFR. Model 1 comprises ≥ 50% stenosis alone (blue line) with an area under the curve (AUC) of 0.61; model 2 contains ≥ 50% stenosis + plaque markers* with an AUC of 0.83, $p = 0.0001$; and model 3 incorporated model 2 + CT-FFR resulting in the highest predictive value with an AUC of 0.93, $p = 0.031$ (*plaque markers: lesion length, remodeling index, non-calcified plaque volume, and napkin-ring sign)

In accordance with prior studies, we demonstrated that cCTA-derived plaque markers are significantly different in lesions showing ischemia compared to non-flow limiting stenoses [6, 19, 25]. We found that lesion length, non-calcified plaque volume, remodeling index, and napkin-ring sign were not only significantly different in ischemia-inducing lesions compared to non-hemodynamically significant stenosis but also showed significant discriminatory value to predict lesion-specific ischemia (lesion length: OR 1.15, $p = 0.037$; non-calcified plaque volume: OR 1.02, $p = 0.007$; remodeling index: OR 1.20, $p = 0.031$; and napkin-ring sign: OR 5.97, $p = 0.014$). These findings are consistent with prior studies by Gaur et al [6] and Diaz-Zamudio et al [26] showing predictive value of non-calcified plaque volume, remodeling

index, and napkin-ring sign. Likewise, Iguchi et al [27] identified lesion length as a valuable predictor of significant coronary stenosis, which was confirmed in our study (lesion length: OR 1.15, $p = 0.037$). Furthermore, recent studies by Dey et al [28] and Benz et al [29] identified contrast density difference as the strongest marker for the prediction of lesion-specific ischemia. However, in the present study, contrast density was not evaluated, which might explain the difference in AUCs between the combination of plaque markers (AUC 0.83) and deep machine learning–based CT-FFR (AUC 0.93).

However, some plaque features such as calcified plaque volume, spotty calcifications, and plaque burden yielded no

Table 5 Diagnostic performance of cCTA-derived plaque markers and CT-FFR for the identification of lesion-specific ischemia

Parameter	Sensitivity	Specificity	PPV	NPV
Lesion length > 21 mm	71% (53–85%)	68% (56–79%)	52% (42–62%)	83% (73–89%)
Non-calcified plaque volume > 132 mm^3	62% (44–78%)	65% (53–76%)	47% (37–57%)	78% (69–85%)
Remodeling index > 1.03	74% (56–87%)	49% (37–62%)	42% (34–49%)	79% (67–87%)
Napkin-ring sign	74% (56–87%)	59% (47–71%)	47% (39–56%)	82% (72–89%)
Stenosis ≥ 50%	88% (73–97%)	33% (22–46%)	40% (35–45%)	85% (68–94%)
CT-FFR ≤ 0.80	82% (66–93%)	94% (86–98%)	88% (73–95%)	92% (84–96%)

PPV positive predictive value, *NPV* negative predictive value

Data presented as percentages (%) with 95% confidence intervals in parentheses

relevant difference between flow-obstructive lesions and non-significant stenosis in our study. Similar results were found in a recent investigation showing that calcified plaque volume is not a significant marker of hemodynamically significant coronary stenoses [26]. Spotty calcifications seem to have a predictive value in risk stratification and outcome prediction which has been demonstrated in recent studies [30–32]. In contrast to our findings where plaque burden showed no difference between flow-obstructive and non-flow-obstructive stenosis, Min et al [4] and Nadjiri et al [33] demonstrated a significant association of plaque extent with hemodynamic significant stenosis and cardiovascular outcome.

CT-FFR has been established to reliably predict lesion-specific ischemia in previous studies [34–36]. Moreover, CT-FFR using an on-site deep machine learning algorithm has been validated to assess hemodynamic significance of coronary stenosis [9, 10]. In our investigation, CT-FFR based on deep machine learning showed predictive value (OR 0.81, $p < 0.0001$) to identify ischemia. Furthermore, CT-FFR provides superior discriminatory value over cCTA and plaque markers. The addition of CT-FFR to visual stenosis grading on cCTA and plaque quantification demonstrated incremental predictive value (AUC 0.93, $p = 0.031$). However, the addition of plaque markers to visual stenosis grading on cCTA and CT-FFR did not improve discriminatory value, which is in line with a previous study by Gaur et al [6].

Semi-automated plaque quantification derived from cCTA provides additional prognostic and predictive value beyond cCTA alone. In combination with CT-FFR, the combined morphological and functional non-invasive assessment of CAD provided by cCTA may become the gatekeeper to invasive coronary angiography. Future developments will likely focus on big data and deep machine learning methods to comprehensively synthetize complete functional and anatomical assessment from non-invasive cCTA testing to parametrically assess the severity of CAD.

This study has several limitations that deserve mention. We performed a retrospective investigation, which is therefore subject to limitations inherent to this study design. A relatively small number of patients were included which may incur a selection bias. Therefore, larger, possibly prospective studies will be necessary to validate our findings. Our results on multivariate analysis may be underpowered by the limited number of observations per variable included [37]. Therefore, this data should only be considered hypothesis-generating. Only patients with at least one invasively quantified stenosis were included. Furthermore, we excluded patients with prior myocardial infarction, coronary intervention, and severely reduced left ventricular ejection fraction. Likewise, we did not systematically correlate our findings on cCTA with an invasive reference standard for intracoronary plaque assessment. However, the semi-automated plaque software

used in the present investigation has been established in previous studies [18, 38]. Furthermore, plaque features were not incorporated into a machine learning–based score but assessed by multivariable logistic regression analysis. Combined assessment of plaque features together with CT-FFR using deep machine learning models may further improve discriminatory power.

In conclusion, this study demonstrates that cCTA-derived plaque markers plaque markers portend predictive value to identify lesion-specific ischemia when compared to cCTA stenosis grading alone and the addition of CT-FFR to plaque markers showed incremental discriminatory power.

Compliance with ethical standards

References

1. Smith SC Jr, Feldman TE, Hirshfeld JW Jr et al (2006) ACC/AHA/SCAI 2005 guideline update for percutaneous coronary intervention: a report of the American College of Cardiology/American Heart Association Task Force on Practice Guidelines (ACC/AHA/SCAI writing committee to update 2001 guidelines for percutaneous coronary intervention). Circulation 113:e166–e286

2. Curzen N, Rana O, Nicholas Z et al (2014) Does routine pressure wire assessment influence management strategy at coronary

angiography for diagnosis of chest pain?: the RIPCORD study. Circ Cardiovasc Interv 7:248–255

3. Tonino PA, De Bruyne B, Pijls NH et al (2009) Fractional flow reserve versus angiography for guiding percutaneous coronary intervention. N Engl J Med 360:213–224

4. Min JK, Feignoux J, Treutenaere J, Laperche T, Sablayrolles J (2010) The prognostic value of multidetector coronary CT angiography for the prediction of major adverse cardiovascular events: a multicenter observational cohort study. Int J Cardiovasc Imaging 26:721–728

5. Dey D, Achenbach S, Schuhbaeck A et al (2014) Comparison of quantitative atherosclerotic plaque burden from coronary CT angiography in patients with first acute coronary syndrome and stable coronary artery disease. J Cardiovasc Comput Tomogr 8:368–374

6. Gaur S, Øvrehus KA, Dey D et al (2016) Coronary plaque quantification and fractional flow reserve by coronary computed tomography angiography identify ischaemia-causing lesions. Eur Heart J 37:1220–1227

7. Bauer RW, Thilo C, Chiaramida SA, Vogl TJ, Costello P, Schoepf UJ (2009) Noncalcified atherosclerotic plaque burden at coronary CT angiography: a better predictor of ischemia at stress myocardial perfusion imaging than calcium score and stenosis severity. AJR Am J Roentgenol 193:410–418

8. Dwivedi G, Liu Y, Tewari S, Inacio J, Pelletier-Galarneau M, Chow BJ (2016) Incremental prognostic value of quantified vulnerable plaque by cardiac computed tomography: a pilot study. J Thorac Imaging 31:373–379

9. Tesche C, De Cecco CN, Albrecht MH et al (2017) Coronary CT angiography-derived fractional flow reserve. Radiology 285:17–33

10. Tesche C, De Cecco CN, Baumann S et al (2018) Coronary CT angiography-derived fractional flow reserve: machine learning algorithm versus computational fluid dynamics modeling. Radiology. https://doi.org/10.1148/radiol.2018171291:171291

11. Benton SM Jr, Tesche C, De Cecco CN, Duguay TM, Schoepf UJ, Bayer RR 2nd (2018) Noninvasive derivation of fractional flow reserve from coronary computed tomographic angiography: a review. J Thorac Imaging 33:88–96

12. D'Agostino RB Sr, Vasan RS, Pencina MJ et al (2008) General cardiovascular risk profile for use in primary care: the Framingham heart study. Circulation 117:743–753

13. Task Force Member, Montalescot G, Sechtem U et al (2013) 2013 ESC guidelines on the management of stable coronary artery disease: the task force on the management of stable coronary artery disease of the European Society of Cardiology. Eur Heart J 34: 2949–3003

14. Cury RC, Abbara S, Achenbach S et al (2016) CAD-RADSTM coronary artery disease - reporting and data system. An expert consensus document of the Society of Cardiovascular Computed Tomography (SCCT), the American College of Radiology (ACR) and the north American Society for Cardiovascular Imaging (NASCI). Endorsed by the American College of Cardiology. J Cardiovasc Comput Tomogr 10:269–281

15. Achenbach S, Ropers D, Hoffmann U et al (2004) Assessment of coronary remodeling in stenotic and nonstenotic coronary atherosclerotic lesions by multidetector spiral computed tomography. J Am Coll Cardiol 43:842–847

16. Maurovich-Horvat P, Schlett CL, Alkadhi H et al (2012) The napkin-ring sign indicates advanced atherosclerotic lesions in coronary CT angiography. JACC Cardiovasc Imaging 5:1243–1252

17. Park HB, Heo R, ó Hartaigh B et al (2015) Atherosclerotic plaque characteristics by CT angiography identify coronary lesions that cause ischemia: a direct comparison to fractional flow reserve. JACC Cardiovasc Imaging 8:1–10

18. Tesche C, Caruso D, De Cecco CN et al (2017) Coronary computed tomography angiography-derived plaque quantification in patients with acute coronary syndrome. Am J Cardiol 119:712–718

19. Tesche C, De Cecco CN, Caruso D et al (2016) Coronary CT angiography derived morphological and functional quantitative plaque markers correlated with invasive fractional flow reserve for detecting hemodynamically significant stenosis. J Cardiovasc Comput Tomogr 10:199–206

20. Voros S, Rinehart S, Qian Z et al (2011) Coronary atherosclerosis imaging by coronary CT angiography: current status, correlation with intravascular interrogation and meta-analysis. JACC Cardiovasc Imaging 4:537–548

21. Itu L, Rapaka S, Passerini T et al (2016) A machine-learning approach for computation of fractional flow reserve from coronary computed tomography. J Appl Physiol (1985) 121:42–52

22. Coenen A, Lubbers MM, Kurata A et al (2015) Fractional flow reserve computed from noninvasive CT angiography data: diagnostic performance of an on-site clinician-operated computational fluid dynamics algorithm. Radiology 274:674–683

23. Scanlon PJ, Faxon DP, Audet AM et al (1999) ACC/AHA guidelines for coronary angiography: executive summary and recommendations. A report of the American College of Cardiology/American Heart Association Task Force on Practice Guidelines (committee on coronary angiography) developed in collaboration with the Society for Cardiac Angiography and Interventions. Circulation 99:2345–2357

24. DeLong ER, DeLong DM, Clarke-Pearson DL (1988) Comparing the areas under two or more correlated receiver operating characteristic curves: a nonparametric approach. Biometrics 44:837–845

25. Hell MM, Dey D, Marwan M, Achenbach S, Schmid J, Schuhbaeck A (2015) Non-invasive prediction of hemodynamically significant coronary artery stenoses by contrast density difference in coronary CT angiography. Eur J Radiol 84:1502–1508

26. Diaz-Zamudio M, Dey D, Schuhbaeck A et al (2015) Automated quantitative plaque burden from coronary CT angiography noninvasively predicts hemodynamic significance by using fractional flow reserve in intermediate coronary lesions. Radiology 276: 408–415

27. Iguchi T, Hasegawa T, Nishimura S et al (2013) Impact of lesion length on functional significance in intermediate coronary lesions. Clin Cardiol 36:172–177

28. Dey D, Gaur S, Øvrehus KA et al (2018) Integrated prediction of lesion-specific ischaemia from quantitative coronary CT angiography using machine learning: a multicentre study. Eur Radiol 28: 2655–2664

29. Benz DC, Mikulicic F, Gräni C et al (2017) Diagnostic accuracy of coronary opacification derived from coronary computed tomography angiography to detect ischemia: first validation versus single-photon emission computed tomography. EJNMMI Res 7:92

30. Motoyama S, Kondo T, Sarai M et al (2007) Multislice computed tomographic characteristics of coronary lesions in acute coronary syndromes. J Am Coll Cardiol 50:319–326

31. Pflederer T, Marwan M, Schepis T et al (2010) Characterization of culprit lesions in acute coronary syndromes using coronary dual-source CT angiography. Atherosclerosis 211:437–444

32. Kolossvary M, Szilveszter B, Merkely B, Maurovich-Horvat P (2017) Plaque imaging with CT-a comprehensive review on coronary CT angiography based risk assessment. Cardiovasc Diagn Ther 7:489–506

33. Nadjiri J, Hausleiter J, Jähnichen C et al (2016) Incremental prognostic value of quantitative plaque assessment in coronary CT angiography during 5 years of follow up. J Cardiovasc Comput Tomogr 10:97–104

34. Koo BK, Erglis A, Doh JH et al (2011) Diagnosis of ischemia-causing coronary stenoses by noninvasive fractional flow reserve computed from coronary computed tomographic angiograms. Results from the prospective multicenter DISCOVER-FLOW (diagnosis of ischemia-causing stenoses obtained via noninvasive fractional flow reserve) study. J Am Coll Cardiol 58:1989–1997

35. Nakazato R, Park HB, Berman DS et al (2013) Noninvasive fractional flow reserve derived from computed tomography angiography for coronary lesions of intermediate stenosis severity: results from the DeFACTO study. Circ Cardiovasc Imaging 6:881–889

36. Nørgaard BL, Leipsic J, Gaur S et al (2014) Diagnostic performance of noninvasive fractional flow reserve derived from coronary computed tomography angiography in suspected coronary artery disease: the NXT trial (analysis of coronary blood flow using CT angiography: next steps). J Am Coll Cardiol 63:1145–1155

37. Kunce JT, Cook DW, Miller DE (1975) Random variables and correlational overkill. Educ Psychol Meas 35:529–534

38. Tesche C, De Cecco CN, Vliegenthart R et al (2016) Coronary CT angiography-derived quantitative markers for predicting in-stent restenosis. J Cardiovasc Comput Tomogr 10:377–383